Phytochemistry, 1975, Vol. 14, pp. 683–693. Pergamon Press. Printed in England.

THE DERIVATION AND USE OF BIOSYNTHETIC INCORPORATION AND DILUTION VALUES

IAIN M. CAMPBELL

Department of Biochemistry, Faculty of Arts and Sciences, University of Pittsburgh, 130 DeSoto Street, Pittsburgh, PA 15261, U.S.A.

(*Received* 7 *April* 1974)

Key Word Index—Time dependence; influence of pathway structure; primary precursors; intermediates; secondary metabolites.

Abstract—Mathematical expressions governing incorporation and dilution values in a simple, three component biosynthetic system are established and used to track the influence of pathway structure and sampling time on the numerical value of these parameters. A more productive manner of using the incorporation concept is suggested.

INTRODUCTION

The concepts of per cent incorporation ($I\%$) and dilution value (D) have proved invaluable in interpreting the results of biosynthetic studies in plants and micro-organisms [1–3]. Intelligently used, the magnitude of each of these parameters in tracer experiments allows metabolic pathways to be mapped. For compound B to be derived *in vivo* from compound A, either directly or via a series of intermediates, it is axiomatic that when A is labelled with isotope and fed to the system making B, the incorporation of A into B ($I_{AB}\%$) must be high (at least $>0{\cdot}1\%$) and the dilution value D_{AB} be low (at least less than $1:10^4$). These important parameters are defined in general terms, thus:

$$I_{AB}\% = \frac{Q_B(t)}{Q_A(t_0)} \times 100 \tag{1}$$

$$D_{AB} = \frac{100}{I_{AB}\%} \times \frac{M_B}{M_A} \tag{2}$$

where $Q_B(t)$ is the total number of isotopic atoms isolated in B at the end of the experiment, $Q_A(t_0)$ is the total number of isotopic atoms added to A at the beginning of the experiment, M_B is the molar steady state pool size of B, M_A is the molar steady state pool size of A, t_0 signifies the beginning of the experiment and t some sampling time. For radioisotopes, equations (1) and (2) reduce to (3) and (4) respectively (sp. act. = specific activity); for stable isotopes to (5) and (6) respectively.

$$I_{AB}\% = \frac{\text{sp. act.}_B(t) \times M_B \times 100}{\text{sp. act.}_A(t_0) \times M_A} \tag{3}$$

$$D_{AB} = \frac{\text{sp. act.}_A(t_0)}{\text{sp. act.}_B(t)} \tag{4}$$

$$I_{AB}\% = \frac{\text{enrichment factor}_B(t) \times M_B \times 100}{\text{enrichment factor}_A(t_0) \times M_A} \tag{5}$$

$$D_{AB} = \frac{\text{enrichment factor}_A(t_0)}{\text{enrichment factor}_B(t)}. \tag{6}$$

Care must be taken in using the above equations (a) not to assume M_A is simply the amount of substance added as tracer, i.e. no account being taken of the endogenous pool of A and (b) to ensure that only "atomic" specific activities, not composite molecular ones, are used in equations (3) and (4) [4].

To date, $I\%$ and D values have been used principally to establish a compound's status as an intermediate in a biosynthetic pathway. The approach has been at best semiquantitative. In this paper we establish functions defining the time dependence of $I\%$ and D. It is shown how pathway structure can influence this dependence. The outlines of a more quantitative and biologically more significant utilization of $I\%$ and D data, are drawn.

METHODS*

Consider a plant metabolic pathway comprising three identifiable components, A, B and C which is in the steady state.† The possible interrelationship of those three components and their relationship to the rest of the metabolism of the plant are summarized in Scheme 1. A is a precursor of the product C, and B is an obligatory intermediate in that pathway. The scheme covers all the eventualities that could be encountered normally in a biosynthetic experiment, viz: (a) the A/B and B/C reactions are reversible; (b) there are routes to C other than through A and B, viz‡ X→C, and other routes to B than through A, viz X→B; (c) both A and B can be part of biosynthetic reactions other than A→B→C, viz X→A→O and X→B→O; and (d) C is further metabolized (or lost into growth media, etc.), viz C→O.

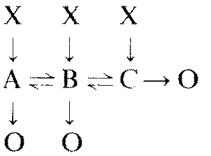

Scheme 1.

* The methods used in this section rely on techniques of compartmental analysis. Excellent articles and monographs on this subject are available [5–14]. Although they relate to more physiological matters, their applicability to plant and fungal biosynthesis is easily projected. The monograph by Shipley and Clark is particularly suitable for bioorganic chemists whose mathematics may be rusty. In this paper the simplest system, compatible with a full development of the topic, is chosen; more complex systems, e.g. a seven component one, can be examined by similar methods (see the latter section of the Appendix for aid in this regard).

† This establishes that there is no (or little) net increase in the size of the pools of A, B and C during the experiment. In practice the duration of the experiment can be selected to make this true.

‡ X and O are used in Scheme 1 and elsewhere to represent generally the rest of the metabolism of the plant or fungus.

§ In this analysis it is essential that pool sizes be in molar terms, as opposed to milligrams etc. Throughout the text we will use mmol units for illustration. This is purely arbitrary, mol, μmol etc. would be equally acceptable. Likewise, we will use the hour as the time unit; seconds or days would be just as good. Note, however, that emergent k values will be in the time unit used initially to define the flow rates.

‖ Mathematically speaking it is more proper to define the flow *from A to B* as F_{BA}, rather than F_{AB}. Operationally, however, the bioorganic chemist will find it more convenient to use the direct form AB. Such is the usage for all vectored subscripted variables in this article.

¶ The k value has been termed in the past, "rate constant", "turnover rate" and "fractional turnover rate". In this article they will be referred to simply as "k values" defined by $k = F/M$.

Let M_A, M_B, and M_C be the molar§ pool sizes of A, B and C respectively, and F_{AB}, F_{BC}, etc. the flow of material *from A to B, from B to C*,‖ etc. per unit time. Let an amount of activity corresponding to $Q_A(t_0)$ isotopic atoms be placed in pool A at $t = 0$. The sp. act. of the A pool at $t = t_0 = 0$ will be $Q_A(t_0)/M_A$. Let the number of isotopic atoms present in pools B and C at time t, by virtue of conversion of A to B to C, be $Q_B(t)$ and $Q_C(t)$ respectively. The sp. act. of pools B and C at time t will be $Q_B(t)/M_B$ and $Q_C(t)/M_C$ respectively.

Expressions for $Q_A(t)$, $Q_B(t)$, $Q_C(t)$ can now be established; the calculation of $Q_A(t)$ serves as an example. The loss of isotope from pool A will correspond to the difference between the outflow of isotope to O and B (see Scheme 1), and the inflow of isotope from B. (Note that although material flows from X to A, this flow brings no isotope with it.) The outflow of isotope from A will equal the product of the mass outflow from A and the specific activity of A; likewise the inflow to A from B will equal the mass flow from B to A multiplied by the sp. act. of B. Hence:

$$-\frac{dQ_A(t)}{dt} = (F_{AO} + F_{AB}) \times \text{sp. act.}_A(t) - F_{BA} \times \text{sp. act.}_B(t). \quad (7)$$

Since $\text{sp. act.}_A(t) = Q_A(t)/M_A$, etc. equation 7 can be re-expressed as:

$$\frac{dQ_A(t)}{dt} = \frac{F_{BA}}{M_B} Q_B(t) - \frac{(F_{AO} + F_{AB})}{M_A} Q_A(t). \quad (8)$$

If k_{BA} is now defined as that proportion of the pool B that transfers to pool A per unit time, i.e. $k_{BA} = F_{BA}/M_B$, and similar "k values" are set up for the other flows,¶ equation (8) simplifies to:

$$\frac{dQ_A(t)}{dt} = k_{BA} Q_B(t) - (k_{AO} + k_{AB}) Q_A(t). \quad (9)$$

Similar differential equations can be obtained from the time course of isotope build-up in pools B and C, viz:

$$\frac{dQ_B(t)}{dt} = k_{AB} Q_A(t) + k_{CB} Q_C(t) - (k_{BO} + k_{BA} + k_{BC}) Q_B(t) \quad (10)$$

and

$$\frac{dQ_C(t)}{dt} = k_{BC} Q_B(t) - (k_{CO} + k_{CB}) Q_C(t). \quad (11)$$

Note the form in each case: $dQ_M(t)/dt$ = (sum of "$k.Q$" products for all pools feeding isotope to M) − (sum of "$k.Q$" products for all pools fed isotope by M).

(Since in the latter of the two sums the Q is a common $Q_M(t)$, the k value is frequently written as k_{MM} and is taken to mean the sum of the k values for every pool M feeds. Thus, in equation (11), $k_{CC} = k_{CO} + k_{CB}$; in equation (10), $k_{BB} = k_{BO} + k_{BA} + k_{BC}$.)

Equations (9–11) can be solved by standard means (see Appendix) for $Q_A(t)$, $Q_B(t)$ and $Q_C(t)$. The solutions are:

$$Q_A(t) = Q_A(t_0) \times \left(\frac{A_1}{e^{g_1 t}} + \frac{A_2}{e^{g_2 t}} + \frac{A_3}{e^{g_3 t}}\right) \quad (12)$$

$$Q_B(t) = Q_A(t_0) \times \left(\frac{B_1}{e^{g_1 t}} + \frac{B_2}{e^{g_2 t}} + \frac{B_3}{e^{g_3 t}}\right) \quad (13)$$

$$Q_C(t) = Q_A(t_0) \times \left(\frac{C_1}{e^{g_1 t}} + \frac{C_2}{e^{g_2 t}} + \frac{C_3}{e^{g_3 t}}\right) \quad (14)$$

where g_1, g_2 and g_3 are the three real roots of the equation:

$$g^3 - (k_{AA} + k_{BB} + k_{CC})g^2 + (k_{AA}k_{BB} + k_{AA}k_{CC} + k_{BB}k_{CC} - k_{AB}k_{BA} - k_{BC}k_{CB})g - (k_{AA}k_{BB}k_{CC} - k_{AA}k_{BC}k_{CB} - k_{CC}k_{AB}k_{BA}). \quad (15)$$

and:

$$A_i = \frac{(-g_i + k_{BB})(-g_i + k_{CC}) - k_{BC}k_{CB}}{(-g_i + g_j)(-g_i + g_k)} \quad (16)$$

$$B_i = \frac{(-g_i + k_{CC})k_{AB}}{(-g_i + g_j)(-g_i + g_k)} \quad (17)$$

and:

$$C_i = \frac{k_{BC}k_{AB}}{(-g_i + g_j)(-g_i + g_k)} \quad (18)$$

$i = 1,3$; g_j and g_k are the two variables of the set (g_1, g_2, g_3) other than g_i.

Functions governing the time dependence of $I_{AB}\%$, $I_{AC}\%$ and the corresponding D values are obtained by combining equations (1) and (2) with (13) and (14) viz:

$$I_{AB}\% = \frac{100\,B_1}{e^{g_1 t}} + \frac{100\,B_2}{e^{g_2 t}} + \frac{100\,B_3}{e^{g_3 t}} \quad (19)$$

$$I_{AC}\% = \frac{100\,C_1}{e^{g_1 t}} + \frac{100\,C_2}{e^{g_2 t}} + \frac{100\,C_3}{e^{g_3 t}} \quad (20)$$

$$D_{AB} = \frac{M_B}{M_A} \div \left(\frac{B_1}{e^{g_1 t}} + \frac{B_2}{e^{g_2 t}} + \frac{B_3}{e^{g_3 t}}\right) \quad (21)$$

$$D_{AC} = \frac{M_C}{M_A} \div \left(\frac{C_1}{e^{g_1 t}} + \frac{C_2}{e^{g_2 t}} + \frac{C_3}{e^{g_3 t}}\right). \quad (22)$$

Substitution of equation (12) into equation (1) yields $I_{AA}\%$ which represents the time course of activity drop-off in the A pool: this can be a very useful parameter as will be seen later.

$$I_{AA}\% = \frac{100\,A_1}{e^{g_1 t}} + \frac{100\,A_2}{e^{g_2 t}} + \frac{100\,A_3}{e^{g_3 t}}. \quad (23)$$

By using equations (19–23) we can now predict the incorporation and dilution values at any sample time in a three component biosynthetic system that correlates with Scheme 1. To use them, only pool sizes and flows need to be specified; these two variables yield the k values in terms of which equations (19–23) are written. An example illustrates this point.

$$X \rightarrow A \rightarrow B \rightarrow C \rightarrow O$$

Scheme 2.

Consider the simplified version of Scheme 1 shown in Scheme 2. Let the pool sizes M_A, M_B, M_C be 1, 5 and 10 mmol respectively and the overall flow rate be 1 mmol/hr, i.e. $F_{XA} = F_{AB} = F_{BC} = F_{CO} = 1$ mmol/hr. Since $k = F/M$, $k_{AB} = 1{\cdot}0$, $k_{BC} = 0{\cdot}2$, and $k_{CO} = 0{\cdot}1$, all hr^{-1}; $k_{AA} = k_{AB}$, $k_{BC} = k_{BB}$, and $k_{CO} = k_{CC}$; all other k's in equations (19–23) are zero. Equation (15) transforms to:

$$g^3 - 1{\cdot}3g^2 + 0{\cdot}32g - 0{\cdot}02 = 0$$

whence*

$$g_1 = 1{\cdot}0; g_2 = 0{\cdot}2; g_3 = 0{\cdot}1.$$

Substitution in equations (16–18) yields:

$$A_1 = 1{\cdot}0; A_2 = A_3 = 0$$

$$B_1 = -1{\cdot}25; B_2 = 1{\cdot}25; B_3 = 0$$

$$C_1 = 0{\cdot}28; C_2 = -2{\cdot}50; C_3 = 2{\cdot}22$$

* A FORTRAN IV program (PDP-11) to compute and plot all the functions contained in this article is available from the author.

Table 1. Input parameters for Figs. 1 to 9

Data for Fig.*	M_A	M_B	M_C	F_{AA}/k_{AA}	F_{AO}/k_{AO}	F_{AB}/k_{AB}	F_{BO}/k_{BO}	F_{BC}/k_{BC}	F_{CB}/k_{CB}	F_{CO}/k_{CO}	F_{AA}/k_{AA}	F_{BB}/k_{BB}	F_{CC}/k_{CC}
1	1·0	5·0	10·0	1·0/— †	0·0/0·0	1·0/1·0	0·0/0·0	1·0/0·2	0·0/0·0	1·0/0·1	1·0/1·0	1·0/0·2	1·0/0·1
2	0·15	0·75	7·5	1·0/—	0·0/0·0	1·0/6·67	0·0/0·0	1·0/1·33	0·0/0·0	1·0/0·67	1·0/6·67	1·0/1·33	1·0/0·67
3	1·0	5·0	10·0	100·0/—	99·0/99·0	1·0/1·0	0·0/0·0	1·0/0·2	0·0/0·0	1·0/0·1	100·0/100·0	1·0/0·2	1·0/0·1
4	1·0	5·0	10·0	10·0/—	0·0/0·0	10·0/10·0	9·0/1·8	1·0/0·2	0·0/0·0	1·0/0·1	10·0/10·0	10·0/2·0	1·0/0·1
5	1·0	5·0	10·0	1·0/—	0·0/0·0	1·0/1·0	0·0/0·0	2·0/0·4	1·0/0·1	1·0/0·1	1·0/1·0	2·0/0·4	2·0/0·2
6	1·0	5·0	10·0	1·0/—	0·0/0·0	1·0/1·0	0·0/0·0	100·0/20·0	99·0/9·9	1·0/0·1	1·0/1·0	100·0/20·0	100·0/10·0
7	1·0	5·0	150·0	1·0/—	0·0/0·0	1·0/1·0	0·0/0·0	1·0/0·2	0·0/0·0	1·0/0·007	1·0/1·0	1·0/0·2	1·0/0·007
8	1·0	0·1	10·0	1·0/—	0·0/0·0	1·0/1·0	0·0/0·0	1·0/10·0	0·0/0·0	1·0/0·1	1·0/1·0	1·0/10·0	1·0/0·1
9	1·0	15·0	10·0	1·0/—	0·0/0·0	1·0/1·0	0·0/0·0	1·0/0·07	0·0/0·0	1·0/0·1	1·0/1·0	1·0/0·07	1·0/0·1

* In all the examples given, F_{BA}, F_{XB}, and F_{XC} are zero. Hence no heading is included for them.
† Since X is indeterminate, k_{XA} has no value.

Table 2. Parameters for equations (19–23) in Figs. 1–9

Data for Fig.	g_1	g_2	g_3	A_1	A_2	A_3	B_1	B_2	B_3	C_1	C_2	C_3
1	1·0	0·2	0·1	1·0	0·0	0·0	−1·25	1·25	0·0	0·28	−2·5	2·22
2	6·67	1·33	0·67	1·0	0·0	0·0	−1·25	1·25	0·0	0·28	−2·5	2·22
3	100·0	0·2	0·1	1·0	0·0	0·0	−0·01	0·01	0·0	0·0	−0·02	0·02
4	10·0	2·0	0·1	1·0	0·0	0·0	−1·25	1·25	0·0	0·02	−0·13	0·11
5	1·0	0·52	0·08	1·0	0·0	0·0	−1·82	1·52	0·3	0·91	−1·88	0·97
6	29·9	1·0	0·07	0·0	1·0	0·0	−0·02	−0·33	0·35	0·02	−0·74	0·72
7	1·0	0·2	0·007	1·0	0·0	0·0	−1·25	1·25	0·0	0·25	−1·29	1·04
8	100·0	10·0	0·1	0·0	1·0	0·0	−0·11	0·11	0·0	0·11	−1·23	1·12
9	1·0	0·1	0·07	1·0	0·0	0·0	−1·07	0·0	1·07	0·08	−2·22	2·14

whence

$$I_{AA}{}^{0}/_{0} = 100/e^{t} \tag{24}$$

$$I_{AB}{}^{0}/_{0} = -125/e^{t} + 125/e^{0\cdot 2t} \tag{25}$$

$$I_{AC}{}^{0}/_{0} = 28/e^{t} - 250/e^{0\cdot 2t} + 222/e^{0\cdot 1t} \tag{26}$$

$$D_{AB} = 5/(-1\cdot 25/e^{t} + 1\cdot 25/e^{0\cdot 2t}) \tag{27}$$

$$D_{AC} = 10/(0\cdot 28/e^{t} - 2\cdot 50/e^{0\cdot 2t} + 2\cdot 22/e^{0\cdot 1t}). \tag{28}$$

RESULTS

Figures 1–9 represent the plots of $I_{AA}{}^{0}/_{0}$, $I_{AB}{}^{0}/_{0}$, $I_{AC}{}^{0}/_{0}$, D_{AB} and D_{AC} against time ($0\cdot 01 < t < 100$) for nine different variations of Scheme 1. Logarithmic scales have been used to accommodate the large range of the variables. From these plots, the general influence of sampling time and pathway structure can be deduced. The flow and pool size values used in generating the figures are collected in Tables 1 and 2. Before examining the traces, it must be emphasized that in every case the A → B → C pathway is an active one; *A and B are* bona fide *precursors of C.*

Figure 1 is the plot of equations (24–28). Several results can be noted from a cursory examination of the traces: (a) $I_{AB}{}^{0}/_{0}$ and $I_{AC}{}^{0}/_{0}$ maximize, but at values (66·9 and 49·4% respectively) significantly less than 100%; (b) D_{AB} and D_{AC} minimize during the experiment (1:7·5 and 1:20·2 respectively). Note that high D_{AC} values can be recorded very early* in the feeding; (c) during the experiment the relative magnitudes of $I_{AB}{}^{0}/_{0}$ and $I_{AC}{}^{0}/_{0}$ reverse. Thus until 5 hr have elapsed, $I_{AB}{}^{0}/_{0} > I_{AC}{}^{0}/_{0}$; thereafter $I_{AB}{}^{0}/_{0} < I_{AC}{}^{0}/_{0}$; (d) a similar reversal takes place with the D values: prior to 8 hr $D_{AC} > D_{AB}$; thereafter, the reverse is the case; (e) there are only specific time zones, or "windows", wherein $I_{AB}{}^{0}/_{0}$ and $I_{AC}{}^{0}/_{0}$ have a magnitude large enough (e.g. greater than 0·1%) to convince the experimenter that A is a precursor of B and/or C: <0·01 to 35 hr in the case of $I_{AB}{}^{0}/_{0}$, 0·1 to *ca* 75 hr in the case of $I_{AC}{}^{0}/_{0}$; and (f) likewise there are limits to the window area wherein D_{AB} and D_{AC} have values less than e.g. $1:10^{4}$, <0·01 to 40 hr for D_{AB}, 0·1 to 79 hr for D_{AC}.

Figure 2 depicts what transpires when, in the simple network of Scheme 2, the pool size values

* Terms such as "early", "late", "short time" and "long time" are relative to the range $10^{-2} < t < 10^{2}$ and to the units in which t is measured.

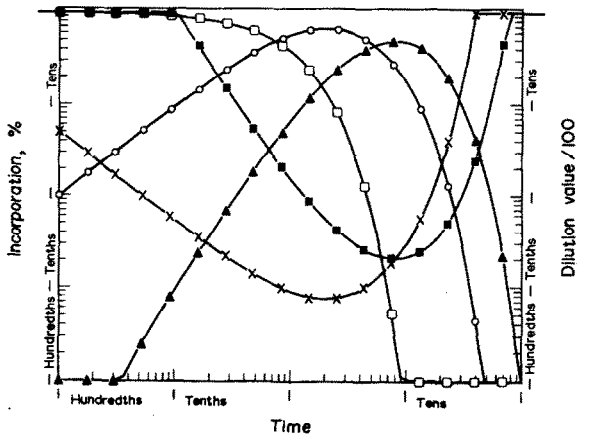

Fig. 1. Time dependence of $I_{AA}\%$ (□—□—□), $I_{AB}\%$ (○—○—○), $I_{AC}\%$ (▲—▲—▲), D_{AB} (×—×—×), and D_{AC} (■—■—■). Values of D in excess of 10^4 have been set equal to 10^4.

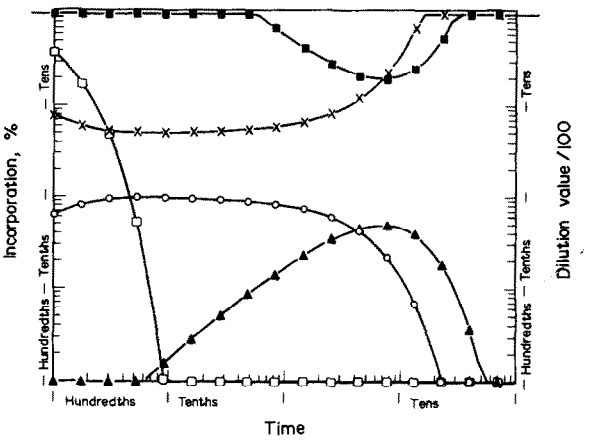

Fig. 3. (See Fig. 1).

are decreased substantially (by 85%), the flows remaining as they were in Fig. 1. The net effect is to increase the k values (see Table 1) and compress the various graphs to the left-hand side of the coordinate system. Thus the maximum value of $I_{AB}\%$ and minimum value of D_{AB} occur at 0·31 hr, the maximum value of $I_{AC}\%$ and minimum value of D_{AC} at 1·26 hr; the corresponding times in Fig. 1 are 2·0 and 7·9 hr respectively. This means the window regions where high $I\%$ and low D values can be recorded, is decreased in size. Whereas sampling in Fig. 1 at 10 hr into the experiment would be fruitful, sampling after a comparable interval in Fig. 2 would be disastrous. The latest time when $I_{AB}\%$ and $I_{AC}\%$ values are in excess of 0·1% in Fig. 2 are 5 and 11 hr respectively.

Comparison of the maximum attainable values of $I_{AB}\%$ and $I_{AC}\%$ and the minimum attainable values of D_{AB} and D_{AC} between Figs. 1 and 2 shows them to be the same. This is a consequence of the fact that, if k values are altered in proportion, the A, B and C factors in equations (19–23) remain the same (see Table 2). Augmentation of the pool sizes in Fig. 1 gives a result analogous but opposite in sense to that of Fig. 2.

Figures 3 and 4 represent a common biosynthetic occurrence. The basic pathway of Scheme 2 is altered to include (a) egress of material from A other than to B (Scheme 3) and (b) egress of material from B other than to C (Scheme 4). The pool sizes are the same as in Fig. 1, as is the net flow of material from A → B → C → O (1·0 mmol/hr). The flow out of the system from A in Fig. 3 has been set to 99·0 mmol/hr, that from B in Fig. 4 to

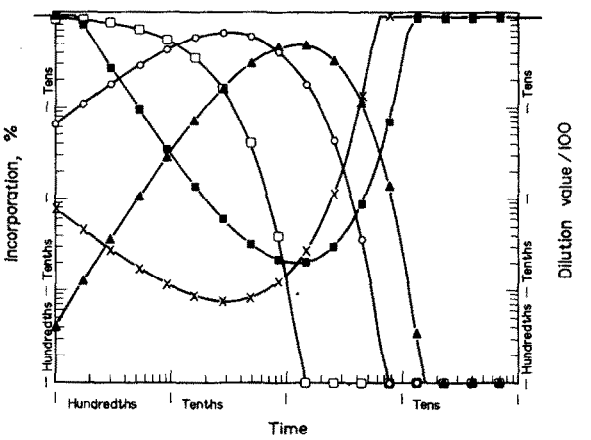

Fig. 2. (See Fig. 1).

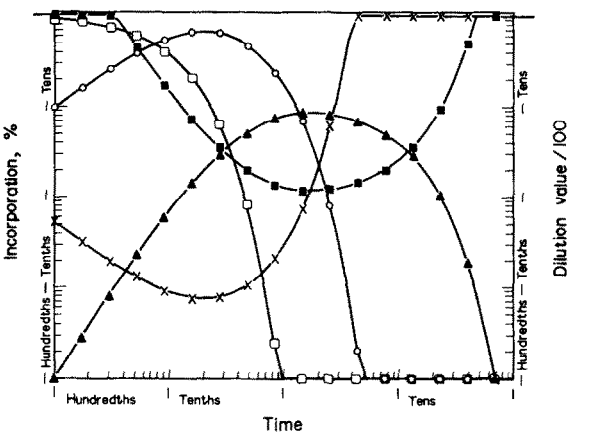

Fig. 4. (See Fig. 1).

$$X \rightarrow A \rightarrow B \rightarrow C \rightarrow O$$
$$\downarrow$$
$$O$$

Scheme 3.

9 mmol/hr. Note from Fig. 3 how precipitously outflow from A reduces the maximum attainable value of both $I_{AB}\%$ and $I_{AC}\%$. The actual values are 0·97 and 0·5% respectively. The corresponding D minimum values are augmented to 1:506 and 1:2000 respectively. Low-D and high-$I\%$ windows diminish in size accordingly. The maximum $I\%$ and minimum D values occur earlier than in Fig. 1, 0·1 hr for A → B, 7·1 hr for A → C.

$$X \rightarrow A \rightarrow B \rightarrow C \rightarrow O$$
$$\downarrow$$
$$O$$

Scheme 4.

Outflow from the intermediate pool B (Fig. 4) produces principally a drop in the maximum value of $I_{AC}\%$ (to 8·5%) and an increase in the minimum value of D_{AC} (to 1:117). The high-$I\%$ and low-D value windows for both A → B and A → C decrease in size as shown by the facts that $I_{AB}\%$ maximizes in 0·2 hr, $I_{AC}\%$ in 1·78 hr. A situation related to schemes 3 and 4, but not presented here in detail involves the synthesis of C by processes which do not involve A or B, i.e. the X → C branch in Scheme 1 is active. It can be shown that in such a system the $I_{AB}\%$ and D_{AB} envelopes overlay completely with those of Fig. 1. The greater the ratio of $k_{XC}:k_{BC}$ the smaller the maximum value of $I_{AC}\%$ now becomes, the larger the minimum value of D_{AC} becomes, and the sooner both occur.

$$X \rightarrow A \rightarrow B \rightleftharpoons C \rightarrow O$$

Scheme 5.

Reversibility of one of the biosynthetic steps is covered in Figs. 5 and 6 (Scheme 5). The pool sizes and net flux A → B → C → O are as in Fig. 1, but in Fig. 5 a reflux of 1 mmol/hr C → B is allowed; in Fig. 6 that reflux is increased to 100 mmol/hr. The small amount of reflux (Fig. 5) causes the high $I\%$ and low D value windows to open significantly. $I\%$ Values in excess of 0·1% are available for A → B from <0·01 to 73 hr, for A → C from 0·08 to 89 hr. The corresponding $D > 1:10^4$ ranges are <0·01 to 89 hr and 0·08 to 99 hr. The maximum values of $I_{AB}\%$ and $I_{AC}\%$ occur earlier than in Fig.

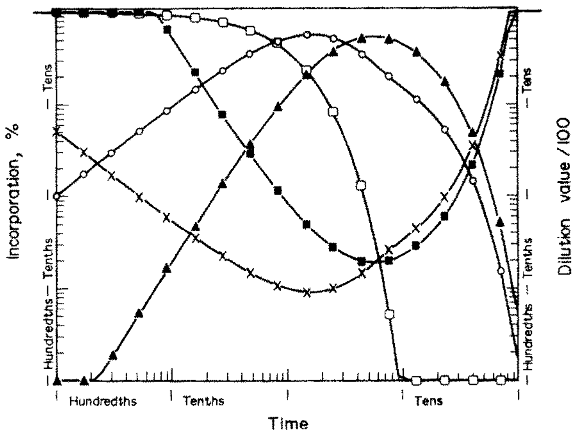

Fig. 5. (See Fig. 1).

1 (1·6 and 5·6 hr respectively) and $I_{AB}\%$ has decreased somewhat to 55·5% with $I_{AC}\%$ increasing proportionately to 53·5%. The more massive reflux occurring in Fig. 6 has a dramatic effect. Acceptable D and $I\%$ values are available over the full time range covered. $I_{AB}\%$ and $I_{AC}\%$ maximize at the same point in time (2·8 hr) and $I_{AC}\%$ (55·0%) is greater than $I_{AB}\%$ (27·5%). The minimum D values for A → B and A → C are both equal (1:18·1), a reflection of the fact that sp. act.$_A$ equals sp. act.$_B$. The maximum $I\%$ values are therefore inversely proportional to the pool sizes.

The remaining plots deal with pool size variations. So far, we have worked with a fixed ratio of $M_A:M_B:M_C$ of 1:5:10. This we now alter, but hold the flow rates constant at 1 mmol/hr. Figure 7 shows the outcome of increasing M_C to 150 mmol, but holding M_A and M_B at 1 and 5 respectively. There is no effect on the A → B para-

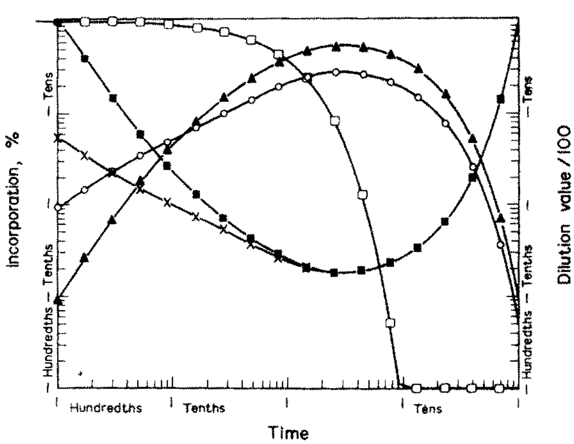

Fig. 6. (See Fig. 1).

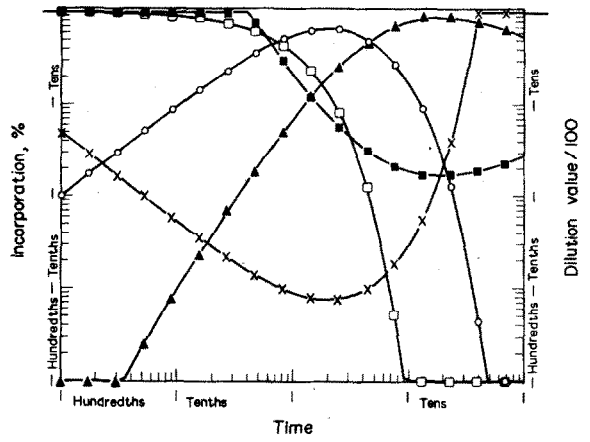

Fig. 7. (See Fig. 1).

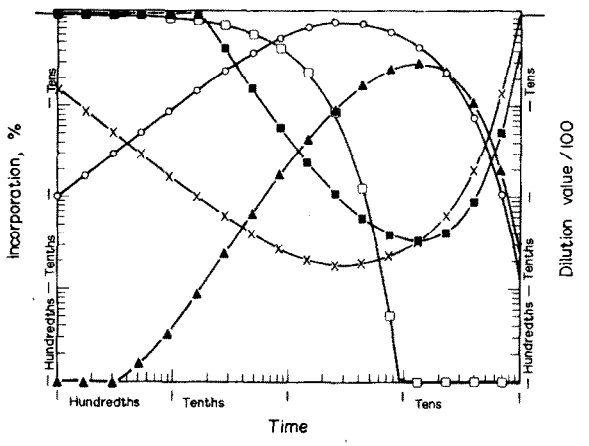

Fig. 9. (See Fig. 1).

meters, but the maximum attainable value of I_{AC}% increases to 88·8%. Note that the minimum D_{AC} values *does not decrease* but increases to 1:169. Acceptable I_{AC}% and D_{AC} values are available from 0·1 and 0·4 hr respectively out to and beyond the 100-hr period examined.

Decreasing the size of the B pool to 0·1 mmol with the A and C pools holding constant at 1 and 10 mmol respectively (Fig. 8) causes the I_{AB}% maximum to occur more rapidly and to be much smaller in magnitude than in Fig. 1 (7·7% at 0·25 hr as opposed to 66·9% at 2 hr). The minimum D_{AB} value, however, drops markedly from 1:7·5 to 1:1·3. The maximum I_{AC}% is larger (77·3%) than in Fig. 1 and it occurs much earlier (2·8 hr *vis-à-vis* 7·9 hr). Further reduction in size of the B pool causes the three component system to collapse to a two component one. The maximum I_{AB}%, minimum D_{AB} values and their occurrence times in a two component system A → B with M_A = 1 mmol, M_B = 10 mmol and F_{AB} = 1 mmol/hr, are 77·4%, 1:12·9 and 2·5 hr respectively.

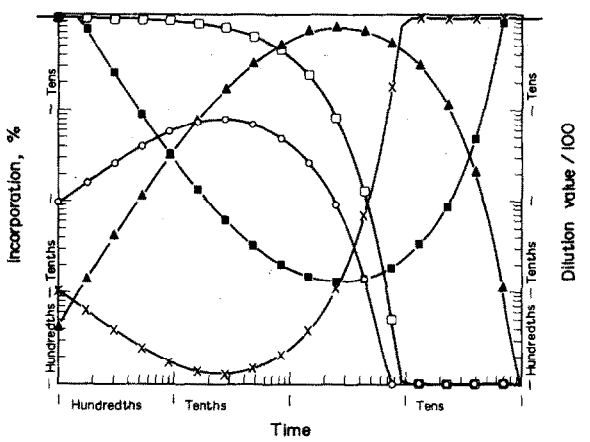

Fig. 8. (See Fig. 1).

In the last trace (Fig. 9) the pool size of the intermediate B is increased to a level in excess of C, viz. 15 mmol. This causes the envelope of I_{AB}% to increase overall; in 2·8 hr the maximum reaches 82·4% and values in excess of 0·1% can be recorded over the whole time range presented. At 1:18·2 the D_{AB} minimum value is comparable to Fig. 1. The A → C parameters suffer accordingly. The maximum I_{AC}% value is 29·5% and it occurs quite late (12·6 hr). The minimum D_{AC} value is 1:34·0. Note, however, that values of D_{AC} in excess of $1:10^4$ are available from a point 0·18 hr into the experiment out to 100 hr and beyond.

One final result can be collected from Figs. 1–9. In each, there are two particular time points, one where I_{AB}% = I_{AC}% and another where D_{AB} = D_{AC}. Where $M_B < M_C$ the I% equality point precedes the D equality point; where $M_B > M_C$ (Fig. 9) the reverse is the case. Note that before either equality point is reached, I_{AB}% > I_{AC}% and $D_{AB} < D_{AC}$; after both are passed, I_{AB}% < I_{AC}% and $D_{AB} > D_{AC}$. In the time zone between the two equality points both I_{AB}% and D_{AB} will be greater than, or less than, I_{AC}% and D_{AC}. The sense will depend on whether $M_B \gtrless M_C$.

DISCUSSION

Several important conclusions can be drawn from this work, based on a simple model though it is. The first is the time-dependent nature of I% and D values. In the natural order of things, I%

starts at zero, maximizes then returns to zero; D starts at infinity, minimizes then returns from whence it came. This is of major significance where "one shot", single sampling experiments are involved. Such studies may paint a bleaker picture than actually exists. The worker may feed the labelled precursor and examine the tissue for intermediates and products before the $I\%$ value for the particular substance has become significant or after it has ceased to be so. Since D values bear a reciprocal relationship to $I\%$ values (equation 2) low $I\%$ results will be accompanied by large D values. The question then becomes: when should sampling occur? If the order of magnitude of the k values is known, the correct time-frame can be predicted and a suitable experiment duration chosen. Unfortunately k values are not usually available. A more practical approach would be to plan to sample the system more than once. This course of action increases the odds of recording meaningful $I\%$ and D data, but it still may be inconclusive; consider the system covered by Fig. 2 sampled at 24, 48, 72 and 96 hr. The analysis here done, however, indicates how such "overshoots" can be avoided. Note how in all the figures, save Fig. 3, the function $I_{AA}\%$ acts as an "internal clock" by which the rest of the metabolic events can be indexed; $I_{AB}\%$ and $I_{AC}\%$ accrue significant value within the time frame in which $I_{AA}\%$ drops to 0·01%. We therefore suggest that it become general practice in biosynthetic experiments to assess the isotopic content of the precursor pool every time a product pool is examined. If the computed $I_{AA}\%$ value is found to be below 0·01%, and no sizeable activity is found in the product pools it can safely be assumed either that the fed precursor bears no direct metabolic relationship to the product, or that its principal biosynthetic role is discharged elsewhere. In both these latter cases poor incorporation data will be forthcoming irrespective of sampling time. $I_{AA}\%$ Assays can be performed by standard techniques of dilution analysis.

A second conclusion from the results of this work is that the maximum obtainable value of $I\%$ is seldom, if ever, 100%. Several factors conspire to make this so, the most fundamental being the continuous nature of the catabolic/anabolic process. From the various figures it can be seen that high $I\%$ values are favored by large pool sizes of the material concerned (Figs. 7 and 9), low pool sizes of any intermediate(s) in the pathway (Fig. 8), and low pool sizes of any products of further metabolism (Fig. 9). Although not actually demonstrated herein, it can be deduced that high $I\%$ values will be recorded where the substance in question accumulates in the tissue or extracellular medium. Under such circumstance no egress occurs from the product pool, i.e. $C \rightarrow 0$ in Scheme 1 is zero.

The minimum attainable values of D are governed in part by the factors, indicated above, that influence $I\%$. As shown in equation (2), however, D is also a function of the ratio, $R = M$ product/M precursor. Hence, in instances where tracer quantities of a precursor are fed in the study of a massively produced secondary metabolite, D will be large even under circumstances where $I\%$ is substantial (see Fig. 7). By the same token, low D values will be encountered for transfer of isotope from a fed major primary metabolite to a small pool of a biosynthetic intermediate (see Fig. 8). In some cases of this type the D value may approach the theoretical lower limit of 1·00.*†

Many biosynthetic experiments involve feeding primary metabolites such as acetate, shikimate, glucose, etc. The results of Figs. 3 and 4 are relevent to such studies. Where fed precursors are preferentially involved in other metabolic networks, low $I\%$ values and large D values can be expected. Bifurcation of the metabolic flow has its greatest influence distal to the branch but a general closing of the high-$I\%$ and low-D windows occurs throughout the pathway. The poor results that emerge do not call in question the integrity of the $A \rightarrow B \rightarrow C \rightarrow O$ pathway; they only demonstrate that the precursor is not exclusively channelled into the product in question.

A valuable conclusion emerging from a comparison of Figs. 1 and 2 is that, provided pool sizes remain the same, slowing down a metabolic process, causes no concomitant drop in the maximum

* The unity lower limit for D applies in radioisotope experiments only where "atomic" sp. act. are used [4]. If a singly labelled precursor is incorporated into a product in a multiple fraction, the ratio: [sp. act. (precursor)]/[sp. act. (product)], i.e. D (equation 4), can in principle drop below 1·00.

† In some experiments, particularly stable isotope labelling ones where relatively large quantities of precursor are fed, there may occur an artificial augmentation of the intracellular precursor pool (M_A in equation 2). Under such circumstances, misleadingly low values for D may be obtained.

attainable value of the various $I\%$ parameters. Hence the probability of culling meaningful $I\%$ and D data should be increased by growing biosynthetic organisms at the lowest possible temperature.

The dissimilarity among Figs. 1–9 underscores the extent to which pathway structure influences $I\%$ and D values. We have already considered the effect of overall biosynthetic rate, the positioning of A and/or B on other competing biosynthetic networks, and, to some extent, the influence of pool sizes of product, precursor and intermediate. In furtherance of this latter point, note from Fig. 8 the approximation that an n pool system containing an intermediate pool of small relative size can be treated as an $(n-1)$ pool system. The influence of reversibility of one of the steps is of interest. In general, reversibility opens the low-D and high-$I\%$ windows (Figs. 5 and 6). Extensive reversibility causes an equilibration of the two pools concerned. This is reflected in an equality of the D values for the pools, and maximum $I\%$ values that are inversely proportional to their pool sizes.

A second concept that emerges from this analysis and that may prove valuable as time-course studies of biosynthesis become more popular, is that of $I\%$ and D equality points (EPs). EPs are important in answering the question: how should the $I\%$ and D parameters of an intermediate relate to those of the product it yields? As described in the last section of the Results the sense of the relationship depends on the position of the sampling time with regard to the EPs and the relative sizes of intermediate and product pools.

At this stage the obvious question arises: if the $I\%$ and D values are so influenced by pathway structure, can they be processed to reveal that structure? In principle, $I\%$ and D time course curves give access to the k values of all the steps in the biosynthetic process, and k values are nothing less than a measure of the *in vivo* activity of the enzyme that is responsible for conducting that particular step. Hence feeding experiments can indicate not only if the fed precursor can be converted to the product in question, but also the rate of that process and the extent to which transfer to the product is in competition with other metabolic outcomes. An approach along those lines has been used by Berman and others [13–17] in studies of the more physiological aspects of mammalian metabolism. A general protocol applicable to plant or fungal metabolism might comprise the following stages: (a) choose a product (P) and some established precursor (A) of that product; (b) feed A to the system and monitor $I_{AA}\%$ and $I_{AP}\%$ as a function of time; (c) check the system for materials that may be intermediates between A and P; (d) if intermediates B and C are found include $I_{AB}\%$, $I_{AC}\%$ measurements in step (b); (e) fit the various $I\%$ vs time curves generated in (b) and (d) to functions of the form:

$$\frac{I\%}{100} = \frac{M_1}{e^{n_1 t}} + \frac{M_2}{e^{n_2 t}} + \frac{M_3}{e^{n_3 t}} \cdots + \frac{M_i}{e^{n_i t}}$$

where $I = 2 +$ number of intermediate pools located in a comprehensive search; and (f) solve for probable k values on the basis of equations such as (15–18) and the parameters M_1, M_2, n_1, n_2, etc, recalling that for $I_{AA}\%$, $\sum M_i = 1$, while for all other $I\%$ functions $\sum M_i = 0$ (see equation xxv in Appendix).

An integrated, analytical hardware combination of a gas chromatograph, mass spectrometer, gas flow proportional counter and digital computer is proving valuable in our hands in collecting the necessary data to allow this hypothetical protocol to be tested [18,19].

APPENDIX

Recall equations (9–11); they are:

$$\frac{dQ_A(t)}{dt} = k_{BA}Q_B(t) - k_{AA}Q_A(t) \quad \text{(i)}$$

$$\frac{dQ_B(t)}{dt} = k_{AB}Q_A(t) + k_{CB}Q_C(t) - k_{BB}Q_B(t) \quad \text{(ii)}$$

$$\frac{dQ_C(t)}{dt} = k_{BC}Q_B(t) - k_{CC}Q_C(t). \quad \text{(iii)}$$

Take the Laplace transform of both sides of equations (i), (ii) and (iii), and set $\mathscr{L}\{Q_A(t)\} = q_A$, $\mathscr{L}\{Q_B(t)\} = q_B$, etc. Hence equations i, ii and iii can be written as:

$$\mathscr{L}\left\{\frac{dQ_A(t)}{dt}\right\} = k_{BA}q_B - k_{AA}q_A \quad \text{(iv)}$$

$$\mathscr{L}\left\{\frac{dQ_B(t)}{dt}\right\} = k_{AB}q_A + k_{CB}q_C - k_{BB}q_B \quad \text{(v)}$$

$$\mathscr{L}\left\{\frac{dQ_C(t)}{dt}\right\} = k_{BC}q_B - k_{CC}q_C. \quad \text{(vi)}$$

Since it is axiomatic that [20]:

$$\mathscr{L}\left\{\frac{df(t)}{dt}\right\} = S.\mathscr{L}\{f(t)\} - f(t=0)$$

where S is the variable of the transform, equations (iv), (v) and (vi) reduce to:

$$S.q_A - Q_A(t_0) = k_{BA}q_B - k_{AA}q_A \quad \text{(vii)}$$

$$S.q_B - 0 = k_{AB}q_A + k_{CB}q_C - k_{BB}q_B \quad \text{(viii)}$$

$$S.q_C - 0 = k_{BC}q_B - k_{CC}q_C \quad \text{(ix)}$$

The left-hand side of each of the above equations results from the fact that $Q_A(t)$ at $t = 0$ is $Q_A(t_0)$—the amount of isotopically labelled atoms added to A initially—but $Q_B(t = 0)$ and $Q_C(t = 0)$ are both zero, i.e. pools B and C initially contained no activity.

Equations (vii), (viii) and (ix) are a set of simultaneous equations in q_A, q_B, q_C of the form:

$$\begin{pmatrix} (S + k_{AA}) & -k_{BA} & 0 \\ -k_{AB} & (S + k_{BB}) & -k_{CB} \\ 0 & -k_{BC} & (S + k_{CC}) \end{pmatrix} \begin{pmatrix} q_A \\ q_B \\ q_C \end{pmatrix} = \begin{pmatrix} Q_A(t_0) \\ 0 \\ 0 \end{pmatrix} \quad \text{(x)}$$

Solutions for q_A, q_B, and q_C come by application of Cramer's rule:

$$q_A = \frac{Q_A(t_0).(S + k_{BB})(S + k_{CC}) - k_{BC}k_{CB}}{\text{DENOM}} \quad \text{(xi)}$$

$$q_B = \frac{Q_A(t_0)(S + k_{CC})k_{AB}}{\text{DENOM}} \quad \text{(xii)}$$

$$q_C = \frac{Q_A(t_0)k_{AB}k_{BC}}{\text{DENOM}} \quad \text{(xiii)}$$

where $\text{DENOM} = (S + k_{AA})[(S + k_{BB})(S + k_{CC}) - k_{BC}k_{CB}] - (S + k_{CC})k_{AB}k_{BA}$.

$Q_A(t)$, $Q_B(t)$ and, $Q_C(t)$ can now be obtained by taking the reverse transform of q_A, q_B and q_C respectively, i.e. of equations (xi), (xii) and (xiii) respectively. Provided these latter three equations can be expressed in the partial fraction form shown below:

$$\frac{q_A}{Q_A(t_0)} = \frac{A_1}{S + g_1} + \frac{A_2}{S + g_2} + \frac{A_3}{S + g_3} \quad \text{(xiv)}$$

$$\frac{q_B}{Q_A(t_0)} = \frac{B_1}{S + g_1} + \frac{B_2}{S + g_2} + \frac{B_3}{S + g_3} \quad \text{(xv)}$$

$$\frac{q_C}{Q_A(t_0)} = \frac{C_1}{S + g_1} + \frac{C_2}{S + g_2} + \frac{C_3}{S + g_3} \quad \text{(xvi)}$$

the solutions are:

$$\frac{Q_A(t)}{Q_A(t_0)} = \frac{A_1}{e^{g_1 t}} + \frac{A_2}{e^{g_2 t}} + \frac{A_3}{e^{g_3 t}} \quad \text{(xvii)}$$

$$\frac{Q_B(t)}{Q_A(t_0)} = \frac{B_1}{e^{g_1 t}} + \frac{B_2}{e^{g_2 t}} + \frac{B_3}{e^{g_3 t}} \quad \text{(xviii)}$$

$$\frac{Q_C(t)}{Q_A(t_0)} = \frac{C_1}{e^{g_1 t}} + \frac{C_2}{e^{g_2 t}} + \frac{C_3}{e^{g_3 t}} \quad \text{(xix)}$$

i.e. equations (12), (13) and (14) of the text.

The appropriate values of g_1, g_2, g_3, A_1, A_2, A_3, B_1, B_2, B_3, C_1, C_2 and C_3 emerge from the operation of partial fraction establishment. Thus, for the right-hand side of equations (xiv) to equal $q_A/Q_A(t_0)$ as defined by equation (xi), the corresponding numerators must be equal, and the denominators equal, i.e.

$$(S + g_1)(S + g_2)(S + g_3) = (S + k_{AA})[(S + k_{BB})(S + k_{CC}) - k_{BC}k_{CB}] - (S + k_{CC})k_{AB}k_{BA} \quad \text{(xx)}$$

and

$$A_1(S + g_2)(S + g_3) + A_2(S + g_1)(S + g_3) + A_3(S + g_1)(S + g_2) = (S + k_{BB})(S + k_{CC}) - k_{BC}k_{CB}. \quad \text{(xxi)}$$

From equation (xx) it follows that:

$$g_1 + g_2 + g_3 = k_{AA} + k_{BB} + k_{CC} \quad \text{(xxii)}$$

$$g_1g_2 + g_2g_3 + g_1g_3 = k_{AA}k_{BB} + k_{BB}k_{CC} + k_{CC}k_{AA} - k_{BC}k_{CB} - k_{BA}k_{AB} \quad \text{(xxiii)}$$

$$g_1g_2g_3 = k_{AA}k_{BB}k_{CC} - k_{AA}k_{BC}k_{CB} - k_{BA}k_{AB}k_{CC}. \quad \text{(xxiv)}$$

From these three conclusions it transpires that g_1, g_2 and g_3 shall be the three real roots of the equation:

$$g^3 - (k_{AA} + k_{BB} + k_{CC})g^2 + (k_{AA}k_{BB} + k_{BB}k_{CC} + k_{AA}k_{CC} - k_{BC}k_{CB} - k_{BA}k_{AB})g - (k_{AA}k_{BB}k_{CC} - k_{AA}k_{BC}k_{CB} - k_{BA}k_{AB}k_{CC})$$

i.e. equation (15) in the text.

From equation (xxi) it follows that:

$$A_1 + A_2 + A_3 = 1 \quad \text{(xxv)}$$

$$A_1(g_2 + g_3) + A_2(g_1 + g_3) + A_3(g_1 + g_2) = k_{BB} + k_{CC} \quad \text{(xxvi)}$$

$$A_1g_2g_3 + A_2g_1g_3 + A_3g_1g_2 = k_{BB}k_{CC} - k_{BC}k_{CB}. \quad \text{(xxvii)}$$

Equations (xxv), (xxvi) and (xxvii) can be expressed in matrix format thus:

$$\begin{pmatrix} 1 & 1 & 1 \\ g_2 + g_3 & g_1 + g_3 & g_1 + g_2 \\ g_2g_3 & g_1g_3 & g_1g_2 \end{pmatrix} \begin{pmatrix} A_1 \\ A_2 \\ A_3 \end{pmatrix} = \begin{pmatrix} 1 \\ k_{BB} + k_{CC} \\ k_{BB}k_{CC} - k_{BC}k_{CB} \end{pmatrix} \quad \text{(xxviii)}$$

whence

$$A_{i,i=1,3} = \frac{(-g_i + k_{BB})(-g_i + k_{CC}) - k_{BC}k_{CB}}{(-g_i + g_j)(-g_i + g_k)}$$

where g_j and g_k are the two variable of the set (g_1, g_2, g_3) other than g_i. A similar type of computation yields the values for B_i and C_i given in text equations (17) and (18).

Should it be required to work with a more complex system than the three component one used in this article, the governing equations can be obtained directly from the matrix equation (x). Notice how the k values are set up about the major diagonal. Columns contain k values for outflow from the pool, rows represent influx of material to the same pool. Positions on the major diagonal are occupied by the sum of S and the total outflow k value. If there is no interaction between two pools (e.g. A and C in the example of the text) the k values corresponding to that location is zero. Extending equation (x) to a 4×4 or even 10×10 is easy to accomplish; the mathematics, however, become a little taxing at higher orders.

Acknowledgements—The author acknowledges with grateful thanks the help and advice of Drs. R. Bently, E. Grotzinger, C. Nulton, J. Slayback, E. McGovern, R. Kadlac and F. Wimberly in preparing this manuscript. The work was performed during tenure of grant number RR 00273 of the U.S. Public Health Service, and grant number P2B4120 of the National Science Foundation.

REFERENCES

1. Swain, T. (1965) in *Biosynthetic Pathways in Higher Plants* (Pridham, J. B. and Swain, T., eds.), p. 9. Academic Press, London.

2. Brown, S. A. (1972) in *Biosynthesis*, Vol. 1, p. 9. The Chemical Society, London.
3. Luckner, M. (1972) in *Secondary Metabolism in Plants and Animals*, p. 15. Academic Press, New York.
4. Campbell, I. M. (1974) *Bioorganic Chemistry* **3,** 386.
5. Aronoff, S. (1956) in *Techniques of Radiobiochemistry*, pp. 75–93. Hefner, New York.
6. Sheppard, C. W. (1962) in *Basic Principles of the Tracer Method*. J. Wiley, New York.
7. Shipley, R. A. and Clark, R. E. (1972) in *Tracer Methods for In Vivo Kinetics*. Academic Press, New York.
8. Jacquez, J. A. (1972) in *Compartmental Analysis in Biology and Medicine*. Elsevier, Amsterdam.
9. Wrenshall, G. A. (1955) *Can. J. Biochem. Physiol.* **33,** 909.
10. Robertson, J. S. (1957) *Physiol. Rev.* **37,** 133.
11. Zilversmit, D. B. (1960) *Am. J. Med.* **29,** 832.
12. Berman, M., Shahn, E. and Weiss, M. F. (1962) *Biophys. J.* **2,** 275.
13. Berman, M., Weiss, M. F. and Shahn, E. (1962) *Biophys. J.* **2,** 289.
14. Baker, N. (1969) *J. Lipid Res.* **10,** 1.
15. Shipley, R. A., Buchwald, E., Chudzik, E. B., Gibbons, A. P., Jongedyk, K. and Brummond, D. O. (1967) *Am. J. Physiol.* **213,** 1149.
16. Baker, N. and Huebotter, R. J. (1972) *J. Lipid Res.* **13,** 716.
17. Samuel, P. and Lieberman, S. (1973) *J. Lipid Res.* **14,** 189.
18. Grotzinger, E. and Campbell, I. M. (1974) *Phytochemistry*, **13,** 923.
19. Campbell, I. M., Grotzinger, E. W., Naworal, J. and Nulton, C. P. (1974) 9th IUPAC International Symposium on the Chemistry of Natural Products, Ottawa, 1974, Abstract C27.